

Evaluation of a 4D Cone-Beam CT Reconstruction Approach using a Simulation Framework

Alexander Hartl and Ziv Yaniv

Abstract—Current image-guided navigation systems for thoracic abdominal interventions utilize three dimensional (3D) images acquired at breath-hold. As a result they can only provide guidance at a specific point in the respiratory cycle. The intervention is thus performed in a gated manner, with the physician advancing only when the patient is at the same respiratory cycle in which the 3D image was acquired. To enable a more continuous workflow we propose to use 4D image data. We describe an approach to constructing a set of 4D images from a diagnostic CT acquired at breath-hold and a set of intraoperative cone-beam CT (CBCT) projection images acquired while the patient is freely breathing. Our approach is based on an initial reconstruction of a gated 4D CBCT data set. The 3D CBCT images for each respiratory phase are then non-rigidly registered to the diagnostic CT data. Finally the diagnostic CT is deformed based on the registration results, providing a 4D data set with sufficient quality for navigation purposes. In this work we evaluate the proposed reconstruction approach using a simulation framework. A 3D CBCT dataset of an anthropomorphic phantom is deformed using internal motion data acquired from an animal model to create a ground truth 4D CBCT image. Simulated projection images are then created from the 4D image and the known CBCT scan parameters. Finally, the original 3D CBCT and the simulated X-ray images are used as input to our reconstruction method. The resulting 4D data set is then compared to the known ground truth by normalized cross correlation(NCC). We show that the deformed diagnostic CTs are of better quality than the gated reconstructions with a mean NCC value of 0.94 versus a mean 0.81 for the reconstructions.

I. INTRODUCTION

The use of image-guided navigation systems has grown in popularity in the past decade, as these systems typically enable procedures that involve substantially less trauma for the patient. To date, these systems have primarily been applied in neurosurgical and orthopedic procedures, as these procedures involve rigid or semi-rigid structures. Interest has now shifted towards systems for thoracic-abdominal interventions [1]. These systems provide guidance based on a three dimensional (3D) image acquired at breath hold, with the intervention performed in a gated manner. That is, the system presents a respiratory signal and tools are advanced only when the signal matches the respiratory phase in which the 3D image was acquired. A more streamlined approach is to use a 4D (3D+time) image synchronized with a respiratory

A. Hartl is with the Imaging Science and Information Systems (ISIS) Center, Dept. of Radiology, Georgetown University Medical Center, Washington, DC, USA, and Chair for Computer Aided Medical Procedures (CAMP), TU Munich, Munich, Germany hartl@in.tum.de

Z. Yaniv is with the Imaging Science and Information Systems (ISIS) Center, Dept. of Radiology, Georgetown University Medical Center, Washington, DC, USA zivy@isis.georgetown.edu

signal. This approach reduces the intervention time and has the potential to improve targeting accuracy.

Recent improvements in flat panel detector technology have resulted in intra-operative C-arm cone-beam CT (CBCT) systems providing reconstructions with soft tissue resolution that is sufficient for interventional purposes [2]. These imaging systems can potentially be used to acquire 4D images with sufficient quality for navigation.

A straightforward approach to the acquisition of 4D CBCT data is to perform gated reconstruction. The acquired projection images are binned according to their respiratory phase with a separate 3D image reconstructed for each bin [3]. For clinical scan times of less than one minute this approach yields images exhibiting reconstruction artifacts due to the spatio-temporal sparseness of the data sampled along the C-arm trajectory and binned according to phase. A theoretical improvement upon this approach was presented in [4]. This approach assumes that a pre-operative 4D motion model is available and that it is consistent with intra-operative respiratory motion. The motion model is incorporated into the reconstruction framework resulting in a 3D motion compensated reconstruction. This approach was later successfully used in the clinical setting, with 1min CBCT gantry rotation and motion models derived from diagnostic 4D CT [5].

In this work we evaluate a registration based approach to deriving a 4D image with sufficient quality for image-guided navigation using a simulation framework. The 4D reconstruction algorithm receives as input a 3D diagnostic CT acquired at breath hold and the set of projective images acquired during the rotation of the CBCT system. Given that this is a simulation study the respiratory phase associated with each projective image is known. In the clinical setting this can be extracted directly from the projective images by analyzing the motion of the diaphragm [5] or from the motion of fiducial markers [6].

We next describe our simulation framework, the proposed 4D CBCT reconstruction method and its evaluation.

II. MATERIALS AND METHODS

All data and acquisition parameters used in this work are based on the Axiom Artis dFA C-arm CBCT system (Siemens AG Healthcare, Erlangen, Germany).

A. Simulated data

To simulate acquisition of a CBCT data set acquired from a free breathing patient we start by acquiring a 3D CBCT image of an anthropomorphic phantom. The phantom is a custom torso constructed from the visible human data [7].

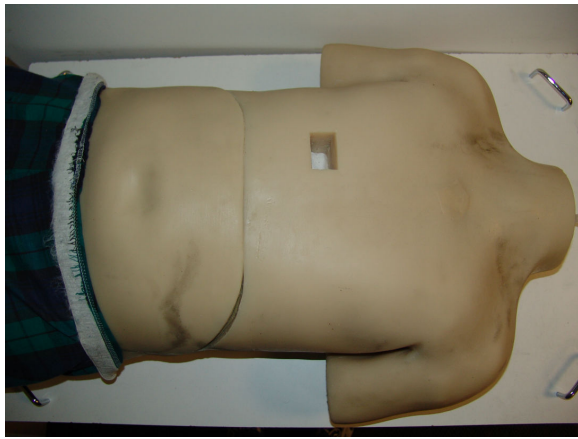


Fig. 1. Anthropomorphic phantom used in this study.

Originally designed for laparoscopic training, it has an abdominal cavity into which synthetic organs can be inserted. In our case we have placed a foam liver model with simulated tumors that are the targets for our image guidance system. The phantom is shown in Figure 1.

To create our ground truth 4D CBCT data set we simulate respiratory motion by deforming the 3D CBCT image. Several methods for simulating deformation are possible: (1) using known motion of a few points that define a sparse displacement field from which a dense deformation field is derived [8]; (2) using registration to infer deformation based on volumetric data sets acquired at breath-hold between end expiration and end inspiration [9] and (3) using finite element methods [10]. The last approach is considered the most accurate as it is based on the physical characteristics of the tissue. In our case we adopted the first approach as it is straightforward to implement and utilizes the data that we currently have available.

To acquire the motion of a few points we used an animal model, under an approved protocol. Four electromagnetically tracked needles were inserted into the animal's liver and tracking data was acquired over multiple respiratory cycles. Based on the positional data we warp the 3D image to create a 4D data set consisting of 3D images at known respiratory phases. The respiratory phase is obtained from one of the tracked fiducials by projecting the fiducial's 3D location onto the principle direction of motion. Figure 2 shows the motion of the four points throughout the respiratory cycle. Figure 3 shows the respiratory signal obtained in this manner.

To obtain a 3D image at a specific respiratory phase we first translate the original 3D image by the mean translation, \bar{t} , obtained from the tracked needles at that phase. We then deform the image using a radial basis function approach as described in [11], with the input being the four residual translations, $t_{\text{residual}_i} = t_i - \bar{t}$. Figure 4 shows coronal slices from three 3D data sets corresponding to simulated end inspiration, mid phase, and end expiration. Ellipse denotes phantom's diaphragm.

Finally, we use our ground truth 4D data to generate a set of simulated projection images, Digitally Reconstructed Radiographs (DRR), simulating a C-arm rotation. The DRRs

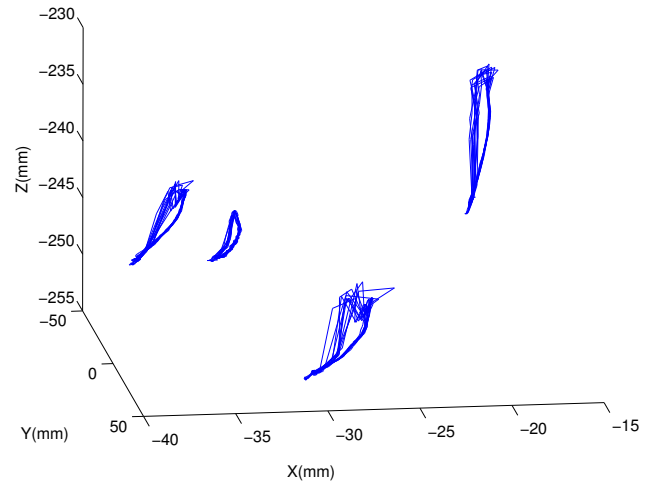


Fig. 2. Motion of electromagnetically tracked needles during respiratory cycle. Hysteresis is clearly visible, the tracked points do not follow the same path during inspiration and expiration.

are generated using the known C-arm projection matrices obtained from our CBCT machine. Respiratory rate is set to 15 breaths per minute, normal tidal breathing. Combined with the knowledge of the C-arm motion this determines which 3D image is used to generate the DRR. Each image is thus time-stamped according to its phase in the respiratory cycle.

It should be noted that the quality of the gated reconstructions is highly dependent on the use of a good spatio-temporal sampling to obtain the projection images. That is, the images for a specific respiratory phase should be evenly distributed along the C-arm trajectory. Initially we simulated the standard clinical soft tissue acquisition protocol, uniformly acquiring 543 images throughout a 220° rotation performed in 20sec . This results in a poor spatio-temporal distribution for motion corresponding to a respiratory rate of 15 breaths per minute, normal tidal breathing, with five respiratory phases, our desired temporal sampling. That is,

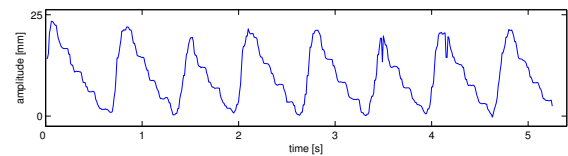


Fig. 3. Respiratory signal obtained from tracked fiducial.

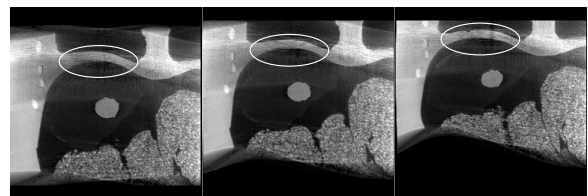


Fig. 4. Coronal slices from three simulated respiratory phases, end inspiration, middle, and end expiration. Ellipse denotes phantom's diaphragm.

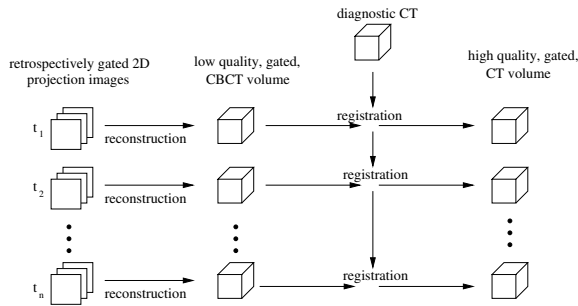


Fig. 5. 4D CBCT reconstruction approach, using a diagnostic CT and intra-operative gated CBCT.

the number of images acquired per respiratory phase is high, but they are clustered into groups along the trajectory and thus contribute little information for reconstruction purposes. Two approaches that improve the spatio-temporal sampling are possible, either slow down the C-arm rotation [5] or acquire multiple acquisitions [12]. In our case we simulated the clinical soft tissue scan, but with a slower C-arm rotation. Instead of a 20sec scan we acquired the same data over 80sec.

B. 4D CBCT reconstruction approach

To perform 4D reconstruction we use a gated reconstruction approach followed by non-rigid registration. As input we receive a set of projection images time-stamped with their respective respiratory phases, and a 3D CBCT image acquired at breath-hold.

We start by performing gated reconstruction. The images are divided into bins according to their respiratory phases and each bin is separately reconstructed using the FDK algorithm [13]. This results in a set of 3D images spanning the respiratory cycle. The quality of these images is lower than that of a 3D reconstruction of a stationary object. This is due to the gating which reduces the number of images used in each reconstruction. While the quality of the reconstruction is not optimal it is sufficient for registration purposes. In our case, we bin the images into five respiratory phases which results in approximately 100 images per bin.

We then non-rigidly register each of the gated reconstructions to the 3D CBCT image acquired at breath-hold. This is done using the multi-resolution diffeomorphic demons method [14]. This registration method is applicable as we are dealing with intra-model registration. In our case we use a six level hierarchy. After registration we deform the 3D breath-hold image to the gated 3D image to obtain a gated image with sufficient quality for navigation. Figure 5 summarizes our reconstruction approach.

III. EVALUATION

To evaluate our approach we use the simulated 4D data set as our ground truth, the simulated projection images and the original 3D CBCT data as a "diagnostic" CT. We then compare each of our 3D reconstructions at the specific respiratory phases to the ground truth volumes using the

	1	2	3	4	5
gated reconstruction	0.81	0.81	0.82	0.81	0.83
after registration	0.93	0.92	0.94	0.94	0.95

TABLE I
NCC VALUES FOR THE FIVE RESPIRATORY PHASES BETWEEN END EXPIRATION (1) AND END INSPIRATION (5).

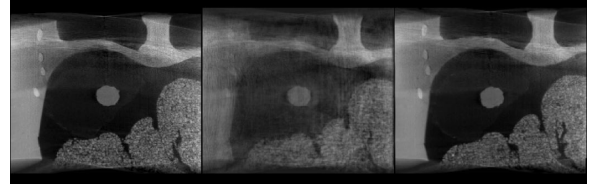


Fig. 6. Coronal slices from: ground truth, gated reconstruction corresponding to same respiratory phase, and registered "diagnostic" CBCT.

Normalized Cross Correlation (NCC), Pearson's r:

$$NCC(I_1, I_2) = \frac{\Sigma(I_1 - \bar{I}_1)(I_2 - \bar{I}_2)}{\sqrt{\Sigma(I_1 - \bar{I}_1)^2 \Sigma(I_2 - \bar{I}_2)^2}}$$

That is, two volumes, I_1 , I_2 , are visually equivalent if they follow a linear relationship. This reflects the standard practice of viewing radiologic images using the window and level linear mapping.

After the initial reconstruction the worst correlation between the gated reconstruction and the corresponding ground truth volume was 0.81, and after registration it was 0.92. Table I and Figure 6 summarize this evaluation.

IV. DISCUSSION

Acquisition of 4D CBCT data using a gating approach without increasing the radiation dose to the patient results in lower quality 3D reconstructions. Effectively replacing artifacts due to respiration with reconstruction artifacts due to insufficient projection data. In this simulation study we utilized a high quality 3D "diagnostic" image in conjunction with lower quality gated CBCT reconstructions to improve the quality of the gated reconstructions.

Our approach is based on the observation that the quality of the gated images is sufficient for registration purposes and that by non-rigidly registering them to a high quality image we can obtain geometrically similar images exhibiting improved visual quality.

Currently, the primary limiting factor in our approach is its computational complexity. Each gated reconstruction and registration take several minutes, multiplied by the number of respiratory phases this becomes clinically infeasible. We will thus investigate the use of graphics processing unit computations to improve the speed of both steps, as this approach has been shown to be highly effective for improving the reconstruction speed [15].

REFERENCES

- [1] T. Peters and K. Cleary, Eds., *Image-Guided Interventions Technology and Applications*. Springer, 2008.

- [2] M. J. Wallace, M. D. Kuo, C. Glaiberman, C. A. Binkert, R. C. Orth, and G. Soulez, "Three-dimensional C-arm cone-beam CT: Applications in the interventional suite," *Journal of Vascular and Interventional Radiology*, vol. 19, no. 6, pp. 799–813, 2008.
- [3] T. Li, L. Xing, P. Munro, C. McGuinness, M. Chao, Y. Yang, B. Loo, and A. Koong, "Four-dimensional cone-beam computed tomography using an on-board imager," *Med. Phys.*, vol. 33, no. 10, pp. 3825–3833, 2006.
- [4] T. Li, E. Schreibmann, Y. Yang, and L. Xing, "Motion correction for improved target localization with on-board cone-beam computed tomography," *Phys. Med. Biol.*, vol. 51, no. 2, pp. 253–267, 2006.
- [5] S. Rit, J. Wolthaus, M. van Herk, and J.-J. Sonke, "On-the-fly motion-compensated cone-beam CT using an a priori motion model," in *Medical Image Computing and Computer-Assisted Intervention*, 2008, pp. 729–736.
- [6] S. Wiesner and Z. Yaniv, "Respiratory signal generation for retrospective gating of cone-beam CT images," in *SPIE Medical Imaging: Visualization, Image-Guided Procedures, and Display*, 2008.
- [7] D. Mazilu *et al.*, "Synthetic torso for training in and evaluation of urologic laparoscopic skills," *J Endourol.*, vol. 20, no. 5, pp. 340–345, 2006.
- [8] F. L. Bookstein, "Principal warps: Thin-plate splines and the decomposition of deformations," *IEEE Trans. Pattern Anal. Machine Intell.*, vol. 11, no. 6, pp. 567–585, 1989.
- [9] T. Rohlfing, C. Maurer, Jr., W. G. O'Dell, and J. Zhong, "Modeling liver motion and deformation during the respiratory cycle using intensity-based free-form registration of gated MR images," *Medical Physics*, vol. 31, no. 3, pp. 427–432, 2004.
- [10] J.-M. Schwartz, M. Denninger, D. Rancourt, C. Moisan, and D. Laurendeau, "Modelling liver tissue properties using a non-linear visco-elastic model for surgery simulation," vol. 9, no. 2, pp. 103–112, 2005.
- [11] Z. Yaniv, R. Stenzel, K. Cleary, and F. Banovac, "A realistic simulation framework for assessing deformable slice-to-volume (CT-fluoroscopy/CT) registration," in *SPIE Medical Imaging: Visualization, Image-Guided Procedures, and Display*, K. Cleary and R. Galloway, Eds. SPIE, 2006, pp. 116–123.
- [12] G. Lauritsch, J. M. Boese, L. Wigström, H. Kemeth, and R. Fahrig, "Towards cardiac C-Arm computed tomography," *IEEE Trans. Med. Imag.*, vol. 25, no. 7, pp. 922–934, 2006.
- [13] L. A. Feldkamp, L. C. Davis, and J. W. Kress, "Practical cone-beam algorithm," *Journal of the Optical Society of America A*, vol. 1, no. 6, pp. 612–619, 1984.
- [14] T. Vercauteren, X. Pennec, A. Perchant, and N. Ayache, "Diffeomorphic demons: Efficient non-parametric image registration," *NeuroImage*, vol. 45, no. 1, Supplement 1, pp. S61 – S72, 2009.
- [15] F. Xu and K. Mueller, "Real-time 3D computed tomographic reconstruction using commodity graphics hardware," *Phys. Med. Biol.*, vol. 52, no. 12, pp. 3405–3420, 2007.